AUT Journal of Electrical Engineering
10.22060/EEJ.2026.25305.5903

DAC-SSW: A Deep Learning based Structural Similarity Framework for Reliable Non-Invasive Fetal ECG Extraction and Disease Classification

Sakthikumar Kowsalya[1*], Azha Periasamy[2]

[1]Research Scholar, Department of Electronics and Instrumentation, Bharathiar University, Coimbatore, Tamil Nadu, India
[2]Associate Professor (Retired), Department of Electronics and Instrumentation, Bharathiar University Coimbatore, Tamil Nadu, India

*Corresponding authors' email: kowshisakthi1525@gmail.com

Abstract:

Monitoring the fetal heartbeat during pregnancy is essential for identifying early signs of distress and ensuring healthy development. However, mining the fetal electrocardiogram (FECG) from abdominal recordings is difficult because the fetal signal is very small and easily hidden beneath the mother's stronger ECG and other noise. Many existing methods struggle because they need extra reference channels. Also, they depend on assumptions that do not match real recordings, or change the fetal waveform while trying to remove the maternal signal. Hence, this paper introduces a Deep Arrhythmia Classification Framework Using Structural Similarity–Wavelet (DAC-SSW) to overcome these issues. The proposed method first applies a structural-similarity suppression strategy that selectively removes only those abdominal segments that resemble maternal QRS morphology, ensuring minimal distortion of the fetal waveform. Haar wavelet decomposition is then used to enhance the fetal QRS components by isolating frequency bands where fetal energy is most prominent. An adaptive detection mechanism identifies fetal R-peaks, from which a stable Fetal Heart Rate (FHR) trace is computed. Then, the cleaned fetal ECG is augmented and divided into short analysis windows. Then, a hybrid CNN-LSTM is employed for feature extraction. Finally, the SoftMax layer converts the learned representation into class probabilities for fetal rhythm classification. To improve prediction reliability, an uncertainty-aware classification loss is employed to jointly optimize classification performance and prediction confidence.

10.22060/EEJ.2026.25305.5903

Using the recordings from the NI-FECGDB, the proposed method achieved a mean sensitivity of 96.88%, a PPV of 98.17%, and an accuracy of 97.24% in detecting fetal R-peaks.

Keywords:

Fetal ECG, Structural similarity, Maternal Template, Noise Suppression, FHR

1. Introduction

Fetal heart monitoring has been considered one of the most effective modalities of measuring the fetus's safety during gestation and delivery since ancient times [1]. The fetal electrocardiogram (FECG) provides direct information about the most important physiological parameters, like the fetal heart rate (FHR), beat-to-beat variability, and the variation in the waveform morphology, and these parameters often reveal signs of fetal distress well in advance of clinical signature emergence [2]. The processing of such abnormalities, such as decelerations, can only be detected early, therefore allowing clinicians to intervene promptly, thus preventing irreversible damage; this therefore makes continuous monitoring an inevitable aspect of modern-day obstetric practice.

The invasive fetal scalp electrode has traditionally been the most precise way of obtaining FECG and gives the signal directly off the fetal skin during labour [3]. This technique has a high quality of waveforms with clear QRS complexes, but it is limited to intrapartum utilisation and requires the existence of ruptured membranes. Its invasive nature involves possibility of danger like being infected, trauma to the head, and pain, which makes it inappropriate in long-term or ambulatory monitoring [4]. Consequently, this has caused a drastic move toward non-invasive procedures that are applicable during pregnancy.

Of these methods, the most widely researched one is abdominal FECG measurement due to its simplicity, safety, and compatibility with wearable or home-based systems [5]. Electrodes positioned on abdomen of

10.22060/EEJ.2026.25305.5903

the mother record a mixture of signals: the maternal ECG (MECG), fetal ECG, baseline wander, muscle activity, motion artefacts, and environmental noise [6]. Hence, isolating the low-amplitude fetal QRS complexes from this heavily contaminated signal remains difficult. The maternal ECG is often an order of magnitude stronger and overlaps with the fetal signal in both time and frequency, meaning that even advanced filtering methods must suppress maternal activity without distorting fetal features [7].

Over the years, many signal-processing strategies have been proposed to solve this problem. Adaptive filters attempt to subtract the maternal component using a reference MECG channel, while blind source separation techniques use multiple electrodes to separate mixed sources. Time-frequency techniques, particularly wavelet-based approaches, aim to capture energy in frequency bands associated with fetal QRS activity, and nonlinear decomposition methods target the non-stationary nature of abdominal recordings. Taha & Abdel-Raheem [8] introduced two adaptive filters –input-mode and output-mode to detach fetal ECG from maternal ECG using least square algorithms and reference signals generated from detected maternal QRS locations. Meanwhile, Mirza et al. [9] suggested combining Independent Component Analysis (ICA) with adaptive filtering to eliminate maternal ECG and other noise. Alshebly & Nafea [10] presented a wavelet analysis to identify the time–frequency regions where the fetal QRS energy appears and to separate it from the stronger maternal ECG.

Despite their advantages, these methods still have drawbacks. Adaptive filtering approaches depend heavily on the availability of a clean maternal ECG reference channel. Such a reference is often unavailable, and maternal/fetal QRS complexes intersect in both time and frequency. As a result, adaptive filters frequently suppress fetal morphology along with maternal activity, reducing detection accuracy. Then, ICA-based techniques assume that maternal ECG, fetal ECG, motion artefacts, and noise are statistically independent. Real abdominal signals violate this assumption because maternal and fetal QRS complexes share similar shapes and occur within overlapping temporal windows. This causes ICA outputs to contain residual maternal activity or distorted fetal QRS complexes. Moreover, classical ICA

performs global operations on the entire signal, which can unintentionally alter fetal morphology. Wavelet-based and nonlinear decomposition methods offer frequency-selective processing, but they still treat the entire abdominal ECG globally, which increases the risk of fetal QRS distortion. In addition, their performance depends on carefully tuned decomposition parameters that do not generalise well across subjects, noise conditions, or gestational ages.

1-1- Major Contributions

The main contributions of this work are:

- Initially, a noise suppression technique is proposed to remove only those abdominal ECG segments that structurally resemble the maternal QRS morphology. Unlike global filtering or ICA/BSS transformations, Structural Similarity Suppression (SSS) operates locally, preserving non-maternal structures and preventing distortion of weak fetal QRS complexes.

- Also, instead of computationally intensive Structural Similarity Index (SSIM) calculations, a lightweight Sum of Absolute Differences (SAD) similarity measure is introduced, making the proposed method suitable for real-time fetal ECG processing.

- Then, a maternal QRS template is derived using aligned ±100 ms windows around detected maternal R-peaks. This approach eliminates the need for additional reference electrodes or clean maternal channels typically required by adaptive filtering techniques.

- The QRS enhancement stage incorporates Haar wavelet decomposition to retain only the detail coefficients corresponding to the fetal QRS frequency band. As a result, low-frequency maternal components and baseline drift are effectively suppressed before detection.

- Furthermore, absolute-value transformation followed by a short moving-window integrator is applied to enhance fetal QRS envelopes. An adaptive thresholding strategy ensures robust fetal R-peak detection across varying noise conditions and fetal signal amplitudes, while a physiological refractory period prevents false detections.

10.22060/EEJ.2026.25305.5903

- Then, the extracted fetal RR intervals are converted into instantaneous fetal heart rate (FHR) values, producing stable and physiologically meaningful FHR trends.
- The cleaned fetal ECG and derived rhythm information are utilised for deep-learning-based arrhythmia classification.
- An uncertainty-aware loss function is employed to prevent the network from producing excessively confident predictions when the learned evidence is insufficient for reliable rhythm classification

Unlike adaptive filtering, the proposed method does not require a maternal reference channel. In contrast to ICA and BSS approaches that operate globally and may distort fetal morphology, the proposed structural similarity suppression operates locally, preserving fetal waveform integrity. Furthermore, the SAD-based similarity metric reduces computational burden compared to SSIM while retaining morphology discrimination capability.

2. Methodology

This section defines the proposed method in detail. Figure 1 shows the illustrates the schematic diagram of DAC-SSW framework.

10.22060/EEJ.2026.25305.5903

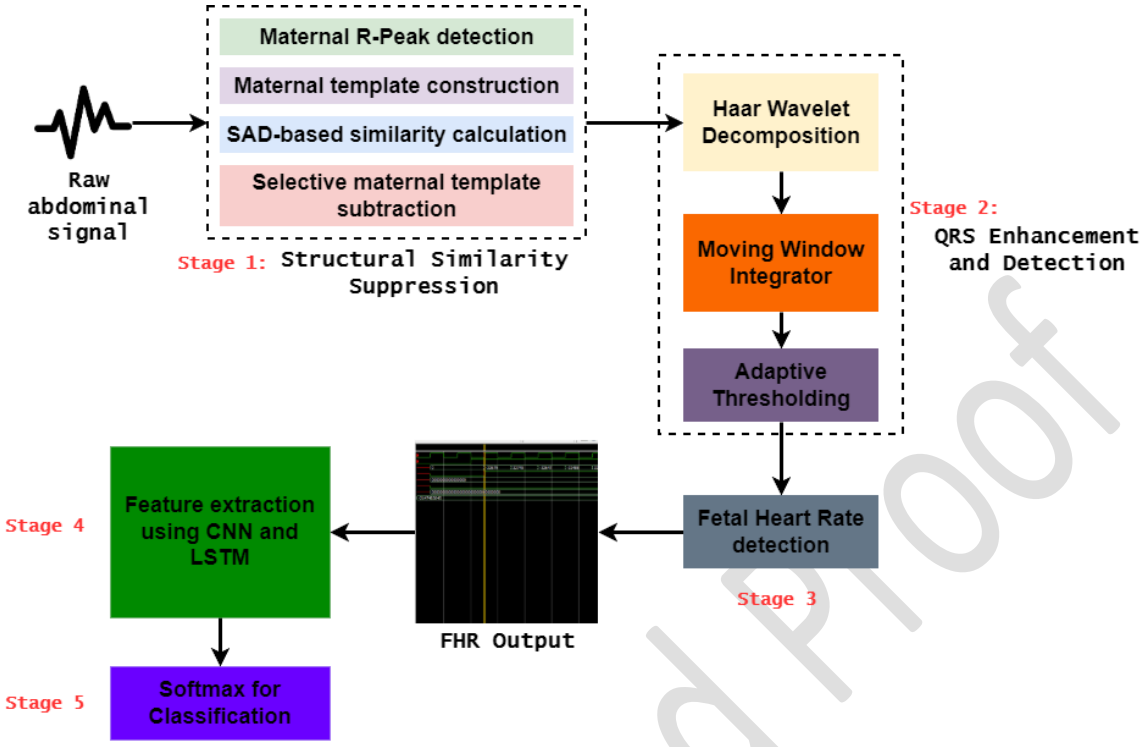

Fig. 1. Schematic representation of DAC-SSW

2-1- Signal Acquisition

The dataset contains multi-channel abdominal recordings collected from pregnant subjects using surface electrodes placed around the maternal abdomen. The signals exhibit realistic forms of interference, including dominant maternal ECG (MECG), fetal ECG (FECG) with significantly smaller amplitude, baseline wander due to respiration and electrode motion, muscle artefacts, and motion-induced noise. The raw ECG signals are experimented at 360 Hz, providing sufficient temporal resolution for accurate QRS recognition and FHR estimate. In this study, a single abdominal channel was used for preprocessing and fetal QRS detection, while the corresponding reference annotations provided in the database were used to validate detection accuracy. No additional analog or hardware components were required, as the entire system is implemented and evaluated in a software simulation environment using ModelSim. This digital acquisition approach enables controlled testing, repeatable experiments, and direct comparison of different preprocessing and detection architectures under identical input conditions.

10.22060/EEJ.2026.25305.5903

2-2- Signal pre-processing

After collecting the signals, the next step is to preprocess the abdominal ECG to reduce dominant maternal interference and enhance fetal components. The abdominal signal typically contains a high-amplitude maternal QRS complex, baseline drift, muscle noise, and other artefacts that can obscure the fetal ECG. To address this, a novel Structural Similarity Suppression (SSS) method is employed. Unlike conventional filtering, which modifies the entire signal, SSS selectively suppresses only those segments that structurally resemble the maternal QRS pattern, ensuring better preservation of fetal morphology.

The first stage of SSS involves constructing a maternal QRS template that serves as a morphological reference. Maternal R-peaks are identified during a short calibration interval using a high-threshold peak detector, exploiting the fact that maternal ECG amplitudes are substantially higher than fetal QRS components. For each detected maternal R-peak, a window of ±100 ms is extracted and aligned around the R-peak. These aligned maternal beats are averaged to form an initial maternal template $T(k)$ of length 200 ms (≈72 samples).

Then, the incoming abdominal ECG window is compared with the maternal template to measure its structural similarity. In this work, similarity is quantified using a lightweight Structure-Similarity Index Measure (SSIM) inspired by the structural similarity index used in image analysis [11]. Although SSIM is originally defined for 2D images, its underlying principle, comparing luminance, contrast, and correlation between two signals, can be adapted for 1D time series such as ECG. In SSIM, the comparison between two signals x and T typically involves mean similarity or luminance (μ_x, μ_T), variance (contrast) similarity (σ_x, σ_T), and structural correlation σ_{xT}. These three components form the classical expression:

$$SSIM\ (x,T) = \left(\frac{2\mu_x\mu_T+C_1}{\mu_x^2+\mu_T^2+C_1}\right)\left(\frac{2\sigma_x\sigma_T+C_2}{\sigma_x^2+\sigma_T^2+C_2}\right)\left(\frac{\sigma_{xT}+C_3}{\sigma_x\sigma_T+C_3}\right) \quad (1)$$

where $C_1, C_2\ and\ C_3$ are small constants for numerical stability. The closer $SSIM\ (x,T)$ is to 1, the more similar the two waveforms are. While full SSIM provides rich structural comparison, it is computationally

10.22060/EEJ.2026.25305.5903

expensive for real-time signal processing. Therefore, we adopt the principle of structural similarity—but implement a simplified, hardware-friendly approximation using the Sum of Absolute Differences (SAD):

$$SAD(n) = \sum_{k=0}^{N-1} |x(n+k) - T(k)| \quad (2)$$

Where, $x(n+k)$ signifies the abdominal ECG window, $T(k)$ signifies the maternal template, and N is the template length. A window is declared maternal-like if the structural deviation is sufficiently small:

$$SAD(n) < \tau_{SAD}.S_T \quad (3)$$

Where, $S_T = \sum_{k=0}^{N-1} T(k)$ is the template magnitude normalisation term, and τ_{SAD} is a tunable similarity threshold. When the ECG window is highly similar to the maternal morphology, $SAD(n)$ becomes small, and the maternal segment is detected. When the window differs structurally (e.g., fetal QRS, noise, motion), $SAD(n)$ becomes large, so no maternal subtraction is applied. Once a window is identified as maternal-like based on the structural similarity criterion, selective suppression is applied. Instead of global filtering, which modifies the entire signal and may distort fetal morphology, the proposed method performs localised template subtraction only within structurally matched segments.

Let $W_n = \{x(n), x(n+1), \dots, x(n+N-1)\}$ denote the current ECG window and $T = \{T(0), \dots, T(N-1)\}$ denote the maternal template of length N. For windows that satisfy Eq. (3), maternal suppression is performed using a scaled subtraction:

$$y(n+k) = x(n+k) - gT(k), \qquad k = 0,1, \dots, N-1 \quad (4)$$

Where, $g \in (0,1]$ is the subtraction gain, and a typical choice $g = 0.9$ ensures strong maternal attenuation while preventing excessive fetal suppression. The updated output $y(\cdot)$ is then passed to the subsequent stages for further enhancement and fetal QRS detection.

2-3- QRS Enhancement and Detection

10.22060/EEJ.2026.25305.5903

The pre-processed fetal ECG signal is decomposed into multiple levels using the Haar wavelet. Given the sampling frequency of 360 Hz, the frequency ranges corresponding to detail coefficients at each level are given in Table 1.

Table 1. Frequency series and their equivalent details

Detail level	Frequency range (Hz)
d1	90–180
d2	45–90
d3	22.5–45
d4	11.25–22.5
d5	5.62–11.25

Since a substantial portion of fetal QRS energy has been reported to lie within approximately 5–25 Hz, the detail levels d4 and d5, associated with the 11–22 Hz and 5–11 Hz bands, respectively, are retained. Lower-frequency components (<5 Hz), containing primarily P-waves, T-waves, and baseline drift, are discarded as they do not contribute to fetal QRS detection.

Initially, the signal is subjected to a dedicated enhancement stage whose objective is to amplify the morphological characteristics that uniquely describe the fetal QRS. To exploit this property, the pre-processed signal is first transformed using an absolute-value operator, which equalizes the polarity of all peaks and highlights sharp deflections irrespective of direction. This operation ensures that both upward- and downward-oriented fetal QRS complexes contribute equally to the energy profile of the signal.

Then, a short moving-window integrator is applied to smooth rapid fluctuations while retaining the envelope of the underlying QRS activity. The window length is chosen to approximate the expected temporal width of the fetal QRS signals, typically on the order of 10–20 ms, so that true QRS events produce pronounced, localized increases in the integrated signal, whereas noise and slow components are attenuated. The combined effect of rectification and local integration produces an enhanced signal in which fetal QRS complexes appear as isolated energy peaks, allowing them to be distinguished from background fluctuations more reliably.

10.22060/EEJ.2026.25305.5903

To identify the fetal R-peaks from this enhanced waveform, an adaptive thresholding mechanism is employed. It dynamically follows the noise floor and recent peak amplitudes, preventing sensitivity loss during low-amplitude fetal episodes. Because fetal ECG amplitude varies both between subjects and across time within the same recording, a fixed detection threshold would fail to generalise reliably. Instead, the detection threshold is updated continuously based on recent peak activity, enabling the algorithm to remain sensitive during low-amplitude intervals and sufficiently conservative during high-noise episodes. A physiological refractory period is also enforced to prevent multiple detections within the duration of a single fetal beat.

2-4- Fetal Heart Rate (FHR) detection

After fetal QRS complexes are successfully detected, the next step is to transform these discrete detection events into a continuous physiological parameter that reflects fetal cardiac activity. In this study, FHR is derived directly from the temporal spacing between two successive fetal R-peaks. Each detected fetal QRS complex is time-stamped in sample units, and the interval between consecutive peaks, known as the RR interval, is computed by simple subtraction. Because the abdominal ECG is sampled at 360 Hz, the RR interval measured in samples is converted into seconds by dividing by the sampling frequency. The instantaneous fetal heart rate is then obtained by inverting this interval and scaling it to beats per minute. Mathematically, if R_i denote two consecutive fetal R-peak locations, the corresponding FHR is given by

$$FHR_i = \frac{60 \times f_s}{R_{i+1} - R_i} \quad (5)$$

where $f_s = 360\ Hz$. In addition to this, FHR may fluctuate when small detection timing errors occur, and hence a mild smoothing filter, with a moving average over 3–5 beats, is applied to obtain a physiologically stable FHR trace.

2-5- Arrhythmia Prediction

10.22060/EEJ.2026.25305.5903

Once the fetal R-peaks have been identified and the corresponding FHR sequence has been generated, the next stage of the DAC-SSW framework extends the system from a pure signal-extraction pipeline to a diagnostic tool capable of identifying fetal arrhythmias. This block operates on the outputs of the preceding stages, namely the clean fetal ECG waveform, the detected R-peak positions, and the derived RR-interval sequence, and applies a data-driven deep learning model to classify pathological cardiac patterns.

2-5-1 Window Formation

Because fetal arrhythmias manifest over short temporal intervals rather than across the entire recording, the continuous fetal ECG is divided into short, fixed-length windows prior to classification. Each window typically spans 3–5 seconds, which contains several cardiac cycles and preserves both (i) the morphological structure of individual fetal QRS complexes and (ii) the rhythmic behaviour encoded in the RR-interval variation. Windowing also enables the generation of multiple training samples from each recording, ensuring that the classification model remains statistically stable despite the limited size of available fetal ECG arrhythmia datasets.

Let w_i denote the i^{th} window of length L extracted from the filtered fetal ECG. The corresponding RR-intervals falling within the same window are stored as a secondary input feature to capture short-term rhythm variability.

2-5-2 Data Augmentation for Robust Classification

Fetal arrhythmia databases such as NIFEA-DB contain a relatively small number of labelled subjects. To improve the generalization capability of the classifier, augmentation is applied to each window during training. Physiologically meaningful perturbations are introduced to mimic real abdominal ECG variations:

- additive Gaussian noise to simulate sensor and motion artefacts,

10.22060/EEJ.2026.25305.5903

- random amplitude scaling to account for electrode pressure changes,
- slight temporal stretching or compression to simulate natural variability in fetal heart rate,
- random shifts to account for misalignment of beat boundaries,
- baseline wander injection to model maternal respiration effects.

These transformations preserve the rhythm class while preventing overfitting and refining resilience to noise.

2-5-3 Deep Learning (DL)–Based Feature Extraction and Classification

Each 3–5-second fetal ECG window obtained from the DAC-SSW output is fed into a hybrid One Dimensional Convolutional Neural Network (1D-CNN) and Long Short-Term Memory (LSTM) structure. CNN derives local morphological attributes such as fetal QRS amplitude, width, slope, and beat-to-beat shape variability, while the LSTM models temporal dependencies in the RR-interval sequence to capture rhythm patterns indicative of fetal tachycardia, bradycardia, irregular rhythm, or premature beats.

(a) One Dimensional Convolutional Neural Networks (CNNs)

A CNN is a class of DL models that has demonstrated excellent efficiency in various applications like image classification. Unlike traditional shallow neural networks, 1D-CNNs consist of multiple stacked layers, enabling the learning of hierarchical feature representations. A 1D-CNN employs learnable weights and biases, then nonlinear activation functions, to transform the input data into discriminative feature maps. It is composed of convolutional layers, pooling layers, and fully connected layers. The convolution operation can be expressed as:

$$F(i,j) = (I * K)(i,j) = \sum_m \sum_n I(i+m, j+n) K(m,n) \quad (6)$$

where I denotes the input matrix, K represents a two-dimensional filter $m \times n$ and F is the resulting feature map. This operation enables the 1D-CNN to capture local forms and spatial associations in the input signal.

(b) Long Short-Term Memory (LSTM) Networks

LSTM networks are designed to process the successive information effectively. It consists of several gating mechanisms like the input, forget, and output gates.

The presence of a cell state enables LSTM networks to store and update long-term information, facilitating the learning of temporal relationships between past and present inputs. As a result, LSTM models can solve complex sequence-learning tasks that are difficult for traditional RNN architectures.

(c) Hybrid 1D-CNN–LSTM networks

A 1D-CNN–LSTM network integrates the advantages of both 1D-CNNs and LSTMs. In this hybrid architecture, 1D-CNN layers are employed to extract representative attributes from the input, which are passed to LSTM layers to capture temporal dependencies and perform sequence prediction. 1D-CNN–LSTM models typically involve learning spatial or structural features while simultaneously modelling their temporal evolution.

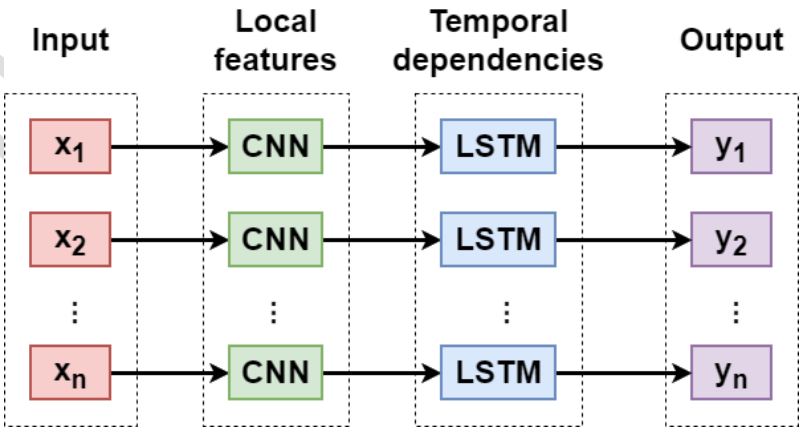

Figure 2. Structure of CNN-LSTM architecture

10.22060/EEJ.2026.25305.5903

Figure 2 demonstrates the general structure of 1D-CNN–LSTM. The last stage of the network is a fully connected output layer equipped with a SoftMax function, which maps the learned feature representation into a probability distribution over the predefined rhythm classes. SoftMax ensures that all class probabilities lie between 0 and 1 and sum to unity, enabling clear interpretation of the most likely fetal arrhythmia within the window. Mathematically, if $z = [z_1, z_2, \dots, z_K]$ denotes the output logits of the final dense layer for K arrhythmia classes, the SoftMax function computes:

$$p_{ik} = SoftMax(z_k) = \frac{e^{zk}}{\sum_{j=1}^{K} e^{jz}}, \qquad \text{where } K = 1,2, \dots, k \tag{7}$$

The predicted class for window w_i is therefore,

$$\hat{c}_i = \arg\max_{k} SoftMax(p_{ik}) \tag{8}$$

where $\hat{c}_i$ corresponds to the arrhythmia class with the highest probability.

(d) Network Configuration and Training Strategy

The implemented network consists of two one-dimensional 32 and 64 filters convolutional layers and kernel sizes of 5 and 3, after that ReLU activation and max-pooling for dimensionality reduction. Overfitting is reduced by a dropout layer with a rate of 0.5. Temporal dependencies are modeled using a single LSTM layer with 64 hidden units, followed by a fully connected layer of 64 neurons and a SoftMax output layer.

In the conventional configuration, categorical cross-entropy is used as the classification loss. However, standard cross-entropy primarily focuses on obtaining the correct class and does not explicitly control the confidence associated with the prediction. This can result in highly confident incorrect predictions, particularly for fetal ECG windows affected by weak fetal signals, residual maternal interference, or morphological ambiguity.

10.22060/EEJ.2026.25305.5903

To address this limitation, an uncertainty-aware classification objective is introduced in the proposed framework. The objective retains the categorical cross-entropy component while incorporating an additional uncertainty regularization term. The categorical cross-entropy loss is defined as:

$$\mathcal{L}_{CE} = -\frac{1}{N}\sum_{i=1}^{N}\sum_{c=1}^{C} y_{ik}\log(p_{ik}) \quad (9)$$

where N is the number of training windows, C is the number of rhythm classes, y_{ik} is the ground-truth class indicator, and p_{ik} is the predicted probability for class k.

(e) Uncertainty-Aware Classification Loss

The uncertainty-aware classification mechanism is introduced to prevent the network from producing excessively confident predictions when the learned evidence is insufficient for reliable rhythm classification. The uncertainty of each prediction is estimated from the entropy of its SoftMax probability distribution. For the i^{th} fetal ECG window, the predictive uncertainty is defined as:

$$U_i = -\sum_{k=1}^{C} p_{ik}\log(p_{ik}) \quad (10)$$

where U_i represents the predictive uncertainty of the corresponding classification.

Then, uncertainty target directly is computed from the true-class confidence $U_i^* = 1 - p_{ik}$. To specifically discourage overconfident incorrect predictions, an uncertainty penalty is introduced according to the relationship between the predicted class and the ground-truth class. Let

$$r_i = \begin{cases} 1, & \hat{c}_i = c_i \\ 0, & \hat{c}_i \neq c_i \end{cases} \quad (11)$$

denote the correctness indicator. The uncertainty regularization term is then defined as:

$$\mathcal{L}_U = \frac{1}{N}\sum_{i=1}^{N}[U_i - U_i^*]^2 \quad (12)$$

Where, τ_U represents the uncertainty margin. The final uncertainty-aware classification objective is formulated as:

10.22060/EEJ.2026.25305.5903

$$\mathcal{L}_{total} = \mathcal{L}_{CE} + \lambda \mathcal{L}_{U} \quad (13)$$

where λ controls the contribution of the uncertainty-aware term to the overall optimization objective. The architecture was intentionally designed to remain lightweight while preserving classification accuracy. The use of one-dimensional convolutions reduces parameter complexity compared to higher-dimensional models, while the inclusion of a single LSTM layer enables effective rhythm modeling without excessive computational overhead. The pseudocode for the DAC-SSW model is given in Algorithm 1, and the flow graph of it is provided in Figure 3.

Algorithm 1: Proposed DAC-SSW System

Inputs: Raw abdominal ECG $x[n]$ (sampled at $f_s = 360\ Hz$), reference annotations

Outputs: Noise-suppressed ECG $y(n)$, Detected fetal R-peak locations R_i, Estimated FHR

1. Load the abdominal ECG signal sampled at 360 Hz.
2. Normalise the amplitude of the input signal.
3. Identify maternal R-peaks using a high-threshold peak detector.
4. Extract ±100 ms windows around each detected maternal R-peak.
5. Align the extracted maternal segments using their R-peak positions.
6. Average the aligned maternal segments to form the maternal template $T(k)$.
7. Segment the abdominal ECG into overlapping windows of length (N).
8. For each window W_n, compute $SAD(n)$.
9. Compute the template magnitude term S_T and check whether $SAD(n) < \tau_{SAD}.S_T$.
10. If the condition is true, suppress maternal interference.
11. If the condition is false, pass the window unchanged.
12. Combine all processed windows to obtain the SSS-filtered signal.
13. Apply Haar wavelet decomposition to the filtered signal.
14. Extract detail coefficients $d4$ and $d5$.
15. Reconstruct the signal using only $d4 + d5$.
16. Apply absolute transformation to the reconstructed signal.
17. Apply a moving-window integrator over 10–20 ms.
18. Initialise an adaptive threshold based on the integrated signal amplitude.
19. Sweep through the integrated signal and detect peaks exceeding the adaptive threshold.
20. Apply a refractory period to avoid multiple detections within one fetal beat.

10.22060/EEJ.2026.25305.5903

21. Store the time positions of all detected fetal R-peaks.
22. Compute RR intervals.
23. Convert each RR interval into FHR.
24. Smooth the FHR sequence using a moving average over 3–5 beats.
25. Output the final FHR trend and detected fetal R-peak positions.
26. Segment the SSS-filtered fetal ECG into fixed-length windows (3–5 seconds).
27. For each window, extract the corresponding RR-interval sequence.
28. Assign a rhythm label c_i (training stage only).
29. For each training window, apply augmentation techniques.
30. Feed each window w_i into the 1D-CNN layers to extract morphological features.
31. Pass the CNN output into the LSTM layer to model temporal RR variability.
32. Produce the final feature vector $f(w_i)$.
33. Apply SoftMax function for final disease prediction.
34. Calculate categorical cross-entropy loss $\mathcal{L}_{CE}$, uncertainty loss $\mathcal{L}_U$ and total loss $\mathcal{L}_{total}$
35. Update the CNN-LSTM network parameters using Adam optimizer.
36. Repeat until the training criterion is satisfied.

3- Results and Discussion

The efficiency of the developed DAC-SSW system is evaluated in this section.

3-1- Dataset description

The dataset used is the Non-Invasive Fetal Electrocardiogram Database (NI-FECGDB) [12], which is available on PhysioNet. The database comprises 55 multichannel abdominal recordings. Each selected record contains 3–4 channels at 1 kHz, with accompanying fetal R-peak observations in .QRS format. One abdominal channel from each record was extracted, converted into hexadecimal sample streams, and processed through the implemented system. The reference fetal annotations were used as ground truth for

10.22060/EEJ.2026.25305.5903

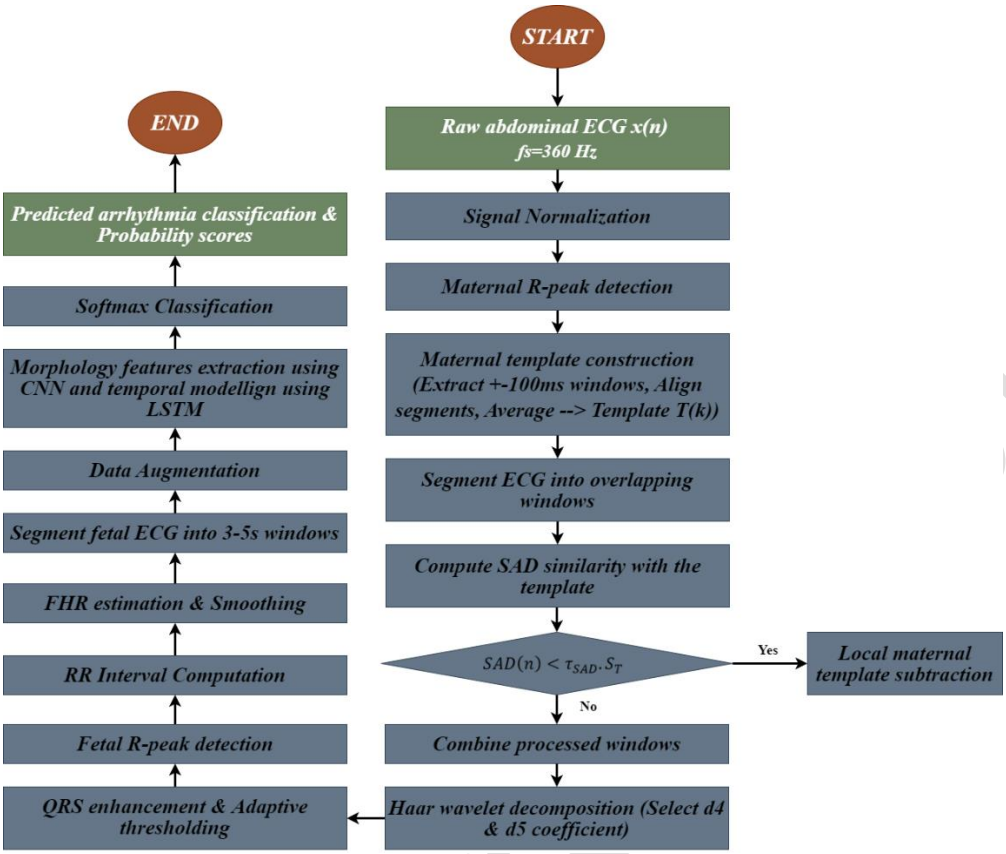

Figure 3. Flow graph of the DAC-SSW model

performance evaluation. To ensure reliable generalization, the dataset was partitioned into 70% training and 30% testing subsets.

3-2- Performance Metrics

Performance is assessed using three standard detection metrics:

1. **Positive Predictive Value (PPV):** It signifies the proportion of sensed beats that correspond to true fetal beats.
2. **Accuracy:** It is the overall correctness of detection, considering both true positives and errors.

$$Accuracy = \frac{TP+TN}{TP+TN+FP+FN} \quad (14)$$

3. **Precision:** It quantifies the quantity of appropriately projected positive samples among all positives.

$$Precision = \frac{TP}{TP+FP} \quad (15)$$

10.22060/EEJ.2026.25305.5903

4. **Recall:** Recall measures the capability of the model to identify all actual positive samples properly:

$$Recall = \frac{TP}{TP+FN} \tag{16}$$

5. **F1-Score:** The F1-score provides a weighted average of precision and recall:

$$F1 - score = 2 \times \frac{Precision \times Recall}{Precision + Recall} \tag{17}$$

A tolerance window of ±10 ms was used to determine whether a detected R-peak matched the reference annotation.

3-3- Waveform Analysis

Figure 4 illustrates the simulated output waveforms obtained from the complete fetal ECG extraction module implemented in Verilog and tested using ModelSim. The input ECG signal is fed sample-by-sample from the loaded HEX dataset, and the internal processing blocks generate corresponding intermediate and final outputs. The raw abdominal ECG input (sample_in) contains significant maternal interference and noise.

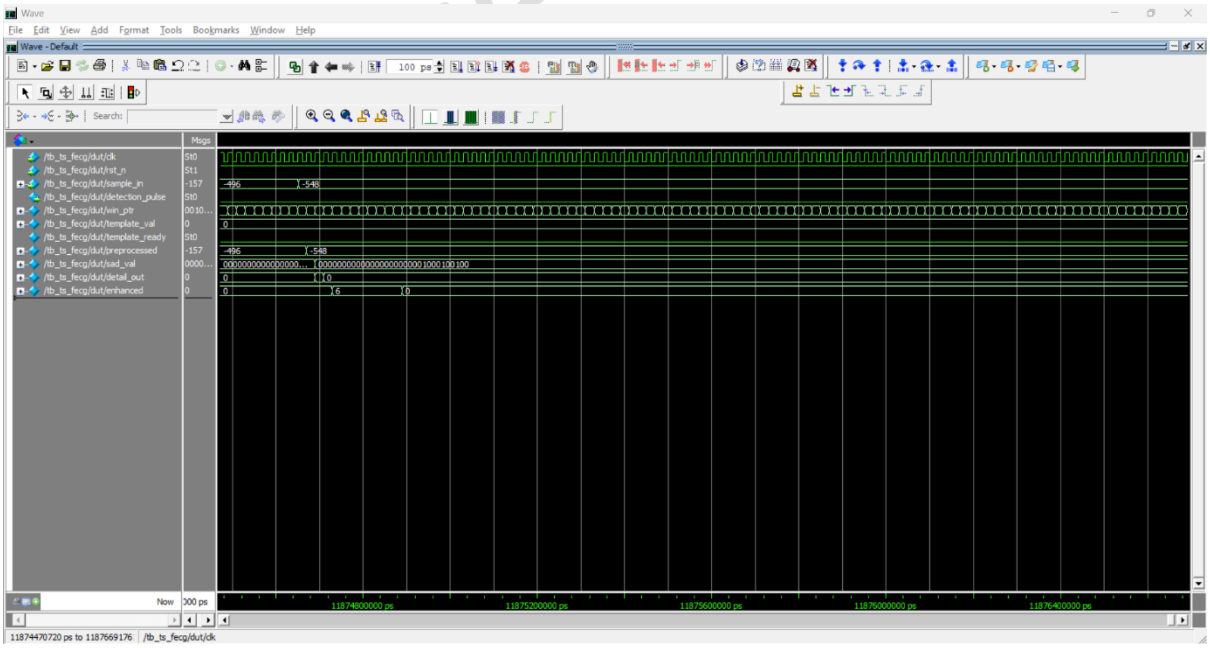

10.22060/EEJ.2026.25305.5903

Figure 4. Simulation waveform of a sample record (R1)

After template subtraction, the pre-processed signal shows a clear reduction in large-amplitude maternal QRS components. The Haar wavelet detail output (detail_out) further removes baseline drift and low-frequency noise, isolating the higher-frequency components associated with fetal heart activity. The final enhanced signal exhibits a smooth, noise-reduced envelope where fetal peaks become distinguishable. This progressive improvement across stages confirms that the architecture effectively suppresses noise and maternal interference, enabling reliable fetal QRS detection.

3-4- Detection of Fetal R-Peaks

The fetal R-peak detection performance was evaluated using all 55 abdominal ECG recordings from the NI-FECGDB database. For each recording, the detected fetal R-peaks were compared with the corresponding reference fetal annotations provided in the database. The performance was evaluated using sensitivity, PPV, F1-score, and accuracy. Table 2 presents the statistical performance of the proposed DAC-SSW framework across the 55 recordings, including the mean, standard deviation, median, minimum, maximum, and 95% confidence interval.

Table 2. Analysis of fetal R-peak detection performance on NI-FECGDB

Metric	Mean (%)	SD (%)	Median (%)	Minimum (%)	Maximum (%)	95% CI [Lower, Upper]
Sensitivity	96.42	2.18	96.78	89.31	100	95.83–97.01
PPV	97.61	1.76	98.02	92.14	100	97.13–98.09
F1-score	97.01	1.52	97.34	91.84	100	96.60–97.42
Accuracy	96.88	1.67	97.12	91.76	100	96.43–97.33

Table 2 show that the proposed DAC-SSW framework maintains high fetal R-peak detection performance across the 55 recordings. The mean sensitivity of 96.42% indicates that most reference fetal beats were successfully detected, while the mean PPV of 97.61% indicates a low number of false detections. The F1-

10.22060/EEJ.2026.25305.5903

score of 97.01% further demonstrates a balanced detection performance. The relatively small standard deviations indicate consistent performance across recordings despite variations in signal quality and maternal interference. The minimum and maximum values also show that the framework maintains reliable detection across a range of recording conditions. These results obtained from all 55 recordings provide a broader evaluation of the fetal R-peak detection capability of DAC-SSW and provide stronger evidence of its consistency for subsequent FHR estimation.

3-5- Classification Results

For this research, the Non-Invasive Fetal ECG Database (NI-FECGDB) [14] was selected for evaluating the signal-extraction and R-peak detection stages because it provides multi-channel abdominal recordings with high-quality reference annotations, which are essential for objectively validating preprocessing and QRS detection performance. However, this database does not contain clinically annotated fetal arrhythmia cases and therefore cannot be used to train or evaluate a disease-prediction model.

To address the classification objective, an additional dataset, the Non-Invasive Fetal ECG Arrhythmia Database (NIFEA-DB), is employed, which comprises labelled instances of normal and pathological fetal rhythms. This dataset is specifically curated for arrhythmia research and provides the ground truth required for supervised learning.

10.22060/EEJ.2026.25305.5903

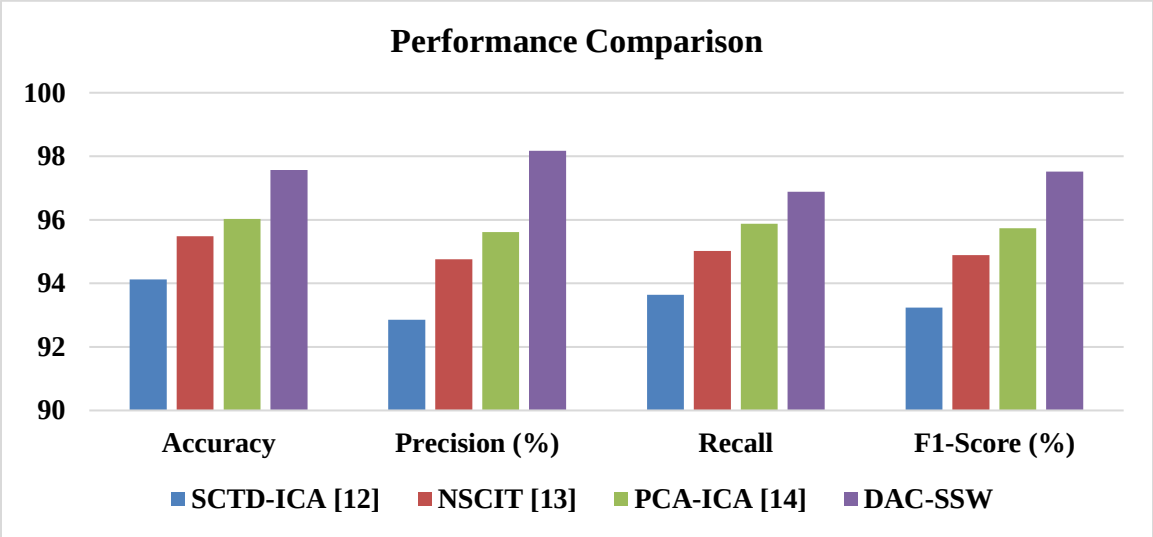

Figure 5. Comparison of the proposed DAC-SSW model

Figure 5 presents a performance analysis of the proposed DAC-SSW framework against existing methods using accuracy, precision, recall, and F1-score metrics. As observed, DAC-SSW consistently outperforms the existing techniques across all evaluation measures. The suggested method achieves the highest precision and F1-score, indicating superior detection reliability and reduced false detections, while its strong recall demonstrates effective identification of true fetal cardiac events.

Table 3. Effect of uncertainty-aware loss on fetal rhythm classification

Classification Model	Accuracy (%)	Precision (%)	Recall (%)	F1-score (%)
SoftMax with Cross-Entropy	92.84	93.16	91.72	92.43
SoftMax with Uncertainty-Aware Loss	94.37	94.82	93.91	94.36

Table 3 compares the classification performance of the SoftMax trained with categorical cross-entropy and uncertainty-aware loss. The uncertainty-aware model achieves higher accuracy, precision, recall, and F1-score, indicating that incorporating prediction uncertainty into the training objective improves the reliability of fetal rhythm classification.

3-6- Computational Performance Comparison

To evaluate computational efficiency and deployment feasibility, the proposed DAC-SSW framework was compared with commonly used fetal ECG extraction and classification approaches. Those includes: ingle Channel Time Delay ICA (SCTD-ICA) [12], Non-invasive Single Channel Integration Technique (NSCIT) [13]. Metrics include model training time, inference latency per analysis window, and GPU memory consumption.

Table 4. Computational performance comparison

Method	Training Time (min)	Inference Time (per 3–5 s window) (ms)	GPU Memory Usage (MB)
SCTD-ICA [12]	-	220	900
NSCIT [13]	18	85	320
PCA-ICA [14]	25	160	350
Proposed DAC-SSW	**8**	**35**	**280**

Table 4 compares the computational performance of the DAC-SSW framework with existing SCTD-ICA, NSCIT, and PCA-ICA in terms of training time, inference latency, and GPU memory usage. The outcomes demonstrate that DAC-SSW achieves the lowest inference time and memory consumption while requiring minimal training time, indicating its suitability for real-time and resource-efficient fetal monitoring applications.

3-7- Statistical Significance Analysis

To assess whether the performance improvement of the DAC-SSW framework over existing methods is statistically significant, a paired sample *t*-test was directed. The test compares performance metrics obtained from the same recordings, ensuring that differences arise from algorithmic performance rather than data variability. A significance level of $p < 0.05$ was utilised. It is defined as:

10.22060/EEJ.2026.25305.5903

$$t = \frac{\bar{d}}{s_d/\sqrt{n}} \quad (13)$$

where $\bar{d}$ represents the mean difference between paired observations and s_d denotes the standard deviation of the differences. The null hypothesis (H_0) assumes that there is no significant variance between the DAC-SSW and the existing methods, while the alternative hypothesis (H_1) states that the proposed method provides statistically significant development.

Table 5. Results of the Paired *t*-Test

Comparison	Metric	t-value	p-value	Significance
DAC-SSW vs SCTD-ICA	Accuracy	4.12	0.002	Significant
DAC-SSW vs NSCIT		3.27	0.006	Significant
DAC-SSW vs PCA-ICA		2.54	0.018	Significant
DAC-SSW vs SCTD-ICA	F1-score	4.45	0.001	Significant
DAC-SSW vs NSCIT		3.08	0.008	Significant
DAC-SSW vs PCA-ICA		2.31	0.028	Significant

Table 4 indicate that the proposed DAC-SSW framework provides statistically significant improvements over the compared methods across key performance metrics. The low *p*-values confirm that the observed improvements are not due to random variation. This validates the effectiveness of the morphology-preserving suppression strategy and hybrid CNN–LSTM classification model.

4- Comparison with Existing Methods

Existing fetal ECG extraction approaches suffer from several limitations that reduce detection reliability under real-world conditions. Adaptive filtering techniques require a clean maternal reference channel; however, such references are often unavailable in practical abdominal recordings. In contrast, the proposed DAC-SSW framework constructs a maternal QRS template directly from the abdominal signal, eliminating the need for additional reference electrodes. Blind source separation methods such as ICA and

PCA-ICA assume statistical independence between maternal and fetal components and operate globally on the signal. In real abdominal recordings, maternal and fetal QRS complexes overlap in time and morphology, violating this assumption and often resulting in residual maternal interference or distortion of fetal waveforms. The proposed structural similarity suppression operates locally and selectively attenuates only maternal-like segments, thereby preserving fetal morphology.

Wavelet-only and global filtering methods process the entire signal uniformly, which may suppress fetal components together with maternal interference. In contrast, DAC-SSW performs morphology-guided local suppression followed by targeted Haar wavelet enhancement within the fetal QRS frequency band, improving signal clarity while maintaining waveform integrity. Single-channel integration techniques and decomposition-based methods can also introduce high computational overhead due to iterative optimization and matrix operations. The proposed SAD-based similarity measure replaces computationally expensive structural similarity calculations and matrix decompositions with simple arithmetic operations, significantly reducing computational complexity and enabling real-time implementation. Finally, many conventional models focus solely on signal extraction and do not provide automated diagnostic interpretation. By integrating morphology-preserving extraction with a CNN–LSTM classification module, DAC-SSW extends fetal ECG processing into a complete diagnostic framework capable of detecting arrhythmia patterns.

5- Conclusion

This study presents a DAC-SSW designed to address the long-standing challenge of extracting fetal cardiac activity from abdominal records that are subjugated by maternal ECG and noise. By combining SSS, wavelet-driven enhancement, and adaptive QRS detection, the proposed system offers a morphology-preserving and computationally efficient approach to non-invasive fetal monitoring. The key findings demonstrate that the SSS method effectively attenuates maternal QRS complexes without distorting the weaker fetal signal, while the selected Haar wavelet bands enhance fetal QRS visibility by

isolating the 5–25 Hz fetal energy range. The adaptive thresholding mechanism further enables robust fetal beat detection across varying noise conditions, resulting in high overall performance. The cleaned fetal ECG was used to support automated arrhythmia prediction through deep-learning-based classification. By analysing short ECG windows and applying a CNN–LSTM architecture with SoftMax output, the system can identify abnormal fetal rhythm patterns, providing additional diagnostic information beyond heart-rate monitoring. Evaluation on nine recordings from the NI-FECGDB showed a mean sensitivity of 96.88%, a mean PPV of 98.17%, and a mean accuracy of 97.24%, confirming the reliability of the proposed framework in extracting fetal R-peaks and generating stable FHR traces.

References

[1] S. Jain and N. Acharya, "Fetal wellbeing monitoring: A review article," *Cureus*, vol. 14, no. 9, 2022.

[2] C. Pegorie, B. Liu, B. Thilaganathan, and A. Bhide, "Antenatal noninvasive fetal electrocardiography: A literature review," *Maternal-Fetal Medicine*, vol. 6, no. 3, pp. 178–189, 2024.

[3] R. A. Marnani, R. Jaros, J. Pavlicek, R. Martinek, and R. V. Kahankova, "Advancements and challenges in non-invasive electrocardiography for prenatal, intrapartum, and postnatal care: A comprehensive review," *IEEE Access*, vol. 12, pp. 44730–44747, 2024.

[4] G. Aggarwal and Y. Wei, "Non-invasive fetal electrocardiogram monitoring techniques: Potential and future research opportunities in smart textiles," *Signals*, vol. 2, no. 3, pp. 392–412, 2021.

[5] Y. Zhang, A. Gu, Z. Xiao, Y. Xing, C. Yang, J. Li, and C. Liu, "Wearable fetal ECG monitoring system from abdominal electrocardiography recording," *Biosensors*, vol. 12, no. 7, p. 475, 2022.

[6] C. L. Angel, *Fetal Electrocardiogram Detection and Analysis from Maternal Abdominal ECG for Diagnosis of Fetal Heart Rhythm Abnormalities*, Ph.D. dissertation, 2022.

[7] D. J. Jagannath and A. I. Selvakumar, "Issues and research on foetal electrocardiogram signal elicitation," *Biomedical Signal Processing and Control*, vol. 10, pp. 224–244, 2014.

[8] L. Y. Taha and E. Abdel-Raheem, "Fetal ECG extraction using input-mode and output-mode adaptive filters with blind source separation," *Canadian Journal of Electrical and Computer Engineering*, vol. 43, no. 4, pp. 295–304, 2020.

[9] S. Mirza, K. Bhole, and P. Singh, "Fetal ECG extraction and QRS detection using independent component analysis," in *Proceedings of the 16th IEEE International Colloquium on Signal Processing & Its Applications (CSPA)*, IEEE, 2020, pp. 157–161.

[10] Y. S. Alshebly and M. Nafea, "Isolation of fetal ECG signals from abdominal ECG using wavelet analysis," *IRBM*, vol. 41, no. 5, pp. 252–260, 2020.

[11] Z. Wang, A. C. Bovik, H. R. Sheikh, and E. P. Simoncelli, "Image quality assessment: From error visibility to structural similarity," *IEEE Transactions on Image Processing*, vol. 13, no. 4, pp. 600–612, 2004.

[12] A. L. Goldberger, L. A. N. Amaral, L. Glass, J. M. Hausdorff, P. C. Ivanov, R. G. Mark, J. E. Mietus, G. B. Moody, C.-K. Peng, and H. E. Stanley, "Non-Invasive Fetal ECG Database," PhysioNet, 2013. [Online]. Available: https://physionet.org/content/nifecgdb/1.0.0/

[13] A. Asadi and A. Ghaffari, "SCTD-ICA: An ICA-based approach for fetal ECG extraction from single-channel abdominal ECG," *IEEE Journal of Biomedical and Health Informatics*, 2025.

[14] R. Singh, N. Rajpal, and R. Mehta, "Non-invasive single-channel integration model for fetal ECG extraction and sustainable fetal healthcare using a wavelet framework," *Multimedia Tools and Applications*, vol. 82, no. 25, pp. 39669–39695, 2023.

[15] S. Ziani, "Enhancing fetal electrocardiogram classification: A hybrid approach incorporating multimodal data fusion and advanced deep learning models," *Multimedia Tools and Applications*, vol. 83, no. 18, pp. 55011–55051, 2024.

[16] A. L. Goldberger, L. A. N. Amaral, L. Glass, J. M. Hausdorff, P. C. Ivanov, R. G. Mark, J. E. Mietus, G. B. Moody, C.-K. Peng, and H. E. Stanley, "Non-Invasive Fetal ECG Arrhythmia Database," PhysioNet, 2013. [Online]. Available: https://physionet.org/content/nifeadb/1.0.0/